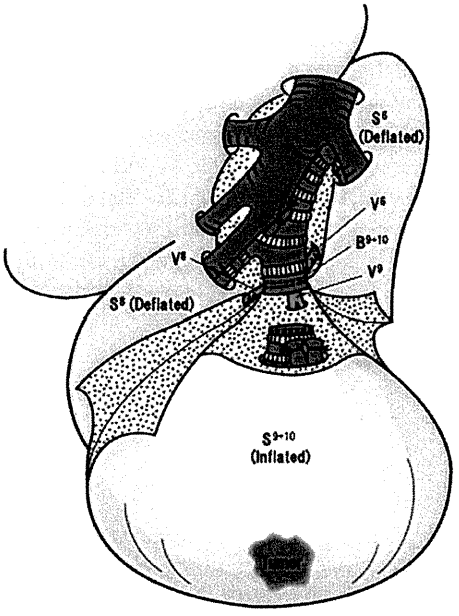

Figure 4. Transection of the central anatomical intersegmental plane made along the intersegmental vein around the hilum. After dissection of B9 + 10, the peripheral stump of B9 + 10 is then lifted, and the anatomical intersegmental plane is used to separate B9 + 10 from the hilum structure. V6, V8, and V9 are separately exposed and taped. The lung parenchyma, along with V6b, V6c, V8a, and V8b, is divided by electrocautery to separate the resected S9 + 10 from the preserved S6 and S8. (Color version of figure is available online at http://www.semthorcardiovascsurg.com.)

ADDITIONAL TECHNICAL PEARLS AND COMMENTS

Key steps for performing radical segmentectomy with lymph node dissection for early-stage non-small cell lung cancer (NSCLC) are as follows: (1) patient selection, (2) hybrid VATS approach, (3) identification of the intersegmental plane by selective jet ventilation, and (4) transection of the intersegmental plane by electrocautery.

Patient Selection

We perform segmentectomy with hilar and mediastinal lymph node dissection for patients with cT1N0 NSCLC of 2 cm or less, even in good-risk patients. When lymph node metastases are evident by frozen section analysis or the resection margin is not sufficient, the surgical procedure must be converted to a lobectomy.

Hybrid VATS Approach

Hilar dissection and intersegmental dissection are performed by using mainly direct visualization through the access thoracotomy (the skin incision is around 50 mm in length), which we call hybrid VATS.[1,2] When the intersegmental plane is being divided by electrocautery, direct visualization during the hybrid VATS approach is extremely important, because a 3-dimensional understanding of the pulmonary anatomy is crucial to avoid ambiguous procedures. We believe that inappropriate segmentectomy is the equivalent of nonanatomical large wedge resection.

Identification of the Intersegmental Plane by Selective Jet Ventilation

We have used a novel method that we developed to detect the intersegmental plane during segmentectomy, which uses selective jet ventilation under bronchofiberscopy.[2] With this method, the segment to be removed can be inflated, while the segments to

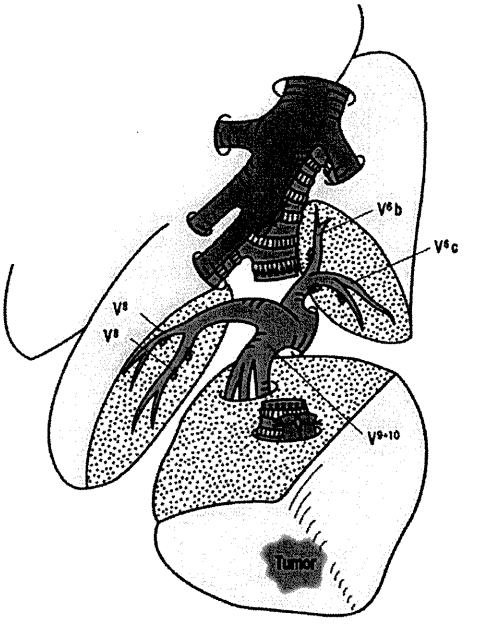

Figure 5. Transection of the intersegmental plane by electrocautery. Transection of the lung parenchyma tissue is then started from the peripheral site along the inflated and deflated line by electrocautery. This peripheral inflation-deflation cutting line must be connected to the central anatomical intersegmental plane made along the intersegmental vein around the hilum. V9 + 10 running toward the inflated S9 + 10 is identified and finally divided. (Color version of figure is available online at http://www.semthorcardiovascsurg.com.)

be preserved are kept deflated. This technique is completely opposite to the conventional method and allows for clear visualization of the anatomical intersegmental line between the segment to be resected and the one to be preserved. We can see the real surgical margin in the inflated segment and obtain a good surgical field because of the small volume of the inflated lung, which does not interfere with the VATS approach.

Transection of the Intersegmental Plane by Electrocautery

Dissection of the intersegmental plane by electrocautery but not staples reduces local failure at the margin. In addition, free cutting (not stapling) of the lung parenchyma is favorable and makes the preserved adjacent segments fully expansive to preserve maximum pulmonary function after the procedure.

1. Okada M, Sakamoto T, Yuki T, et al: Hybrid surgical approach of video-assisted minithoracotomy for lung cancer: Significance of direct visualization on quality of surgery. Chest 128:2696-2701, 2005
2. Okada M, Mimura T, Ikegaki J, et al: A novel video-assisted anatomic segmentectomy technique: Selective segmental inflation via bronchofiberoptic jet followed by cautery cutting. J Thorac Cardiovasc Surg 133:753-758, 2007

Original Article

Steroid Receptor Expression in Thymomas and Thymic Carcinomas

Takahiro Mimae, MD[1,2,3,4]; Koji Tsuta, MD, PhD[1]; Fumiaki Takahashi, ScD[5]; Akihiko Yoshida, MD[1]; Tadashi Kondo, MD, PhD[2]; Yoshinori Murakami, MD, PhD[4]; Morihito Okada, MD, PhD[3]; Masahiro Takeuchi, PhD[5]; Hisao Asamura, MD, PhD[6]; and Hitoshi Tsuda, MD, PhD[1]

BACKGROUND: Although protein expressions of glucocorticoid receptor (GR), estrogen receptors (ERα and ERβ), progesterone receptor A (PgR-A), and androgen receptor (AR) were shown to play roles in the growth and differentiation of normal thymus and thymic tumors, to the authors' knowledge their association with patient characteristics and prognosis has yet to be determined. **METHODS:** A series of 140 thymic epithelial tumors (57 type A + AB thymomas, 40 type B1 + B2 thymomas, 6 type B3 thymomas, and 37 thymic carcinomas) were examined for GR, ERα, ERβ, PgR-A, and AR expression using immunohistochemistry. In addition, the correlation between expression of these hormone receptors and clinicopathologic factors and overall survival (OS) was assessed. **RESULTS:** GR and ERβ demonstrated a high rate of expression in thymomas and thymic carcinomas (82.9% and 76.4%, respectively), whereas rates of ERα, PgR-A, and AR expression were low (13.6%, 0.71%, and 23.6%, respectively). A significant correlation ($P < .05$) was found between ERα expression and tumor size and between ERβ expression and tumor stage. Multivariate analyses revealed that histologic subtype ($P = .0039$), tumor stage ($P = .0012$), and GR expression ($P = .0025$) were significantly correlated with the 10-year OS rate. **CONCLUSIONS:** GR and ERβ demonstrated high rates of expression in thymomas and thymic carcinomas. Furthermore, multivariate analysis revealed that GR expression was associated with better prognosis in patients with surgically resected thymomas and thymic carcinomas. *Cancer* **2011;117:4396–405.** © *2011 American Cancer Society.*

KEYWORDS: glucocorticoid receptor, estrogen receptor, progesterone receptor, thymoma, thymic carcinoma.

Thymomas and thymic carcinomas, the most common epithelial tumors of the anterior mediastinum, are comprised mainly of various percentages of lymphocytes and epithelial cells. The normal thymus is primarily comprised of lymphocytes and thymic epithelial cells. These lymphocytes are comprised mainly of immature T cells called thymocytes. During T-cell ontogeny in the thymus, thymocytes undergo a process of positive (maturation) or negative (apoptosis) selection. Epithelial cells play an active role in promoting T-cell maturation, either through the action of their humoral substances or through direct contact with thymocytes.

Glucocorticoids (GCs), a class of steroid hormones, are important regulatory molecules that control inflammation, cell growth, and differentiation through the activity of a specific intracellular glucocorticoid receptor (GR).[1-3] In the normal thymus, GR is expressed in not only immature thymocytes but also epithelial cells.[4,5] In thymomas, GR expression is also observed in both epithelial cells and lymphocytes by immunohistochemical analysis.[4] The administration of GCs induces apoptosis in thymocytes.[6] The administration of prednisone, the most potent GC, has demonstrated dramatic responses in patients with refractory thymoma.[7-13]

Other steroids such as estrogen or progesterone regulate cell proliferation and other biological functions in various neoplasms derived from hormone-dependent tissues, such as breast and endometrial cancers.[14] These biological effects are in general mediated through initial interactions with native receptors. Estrogen receptor (ER) and progesterone receptor (PgR), 2 representative sex steroid receptors, have been detected in homogenates of the mature human thymus.[15,16] In

Corresponding author: Koji Tsuta, MD, PhD, Division of Pathology, National Cancer Center Hospital, 1-1 Tsukiji 5-chome, Chuo-ku, Tokyo 104-0045, Japan; Fax: (011) 81-3-3545-3567;; ktsuta@ncc.go.jp

[1]Pathology and Clinical Laboratory Division, National Cancer Center Hospital, Tokyo, Japan; [2]Proteome Bioinformatics Project, National Cancer Center Research Institute, Tokyo, Japan; [3]Department of Surgical Oncology, Research Institute for Radiation Biology and Medicine, Graduate School of Biomedical Sciences, Hiroshima University, Hiroshima, Japan; [4]Division of Molecular Pathology, Institute of Medical Science, University of Tokyo, Tokyo, Japan; [5]Department of Clinical Medicine (Biostatistics), School of Pharmacy, Kitasato University, Tokyo, Japan; [6]Division of Thoracic Surgery, National Cancer Center Hospital, Tokyo, Japan

We would like to thank Sachiko Miura and Chizu Kina for their skillful technical assistance.

DOI: 10.1002/cncr.26061, **Received:** October 21, 2010; **Revised:** December 27, 2010; **Accepted:** January 31, 2011, **Published online** March 22, 2011 in Wiley Online Library (wileyonlinelibrary.com)

addition, previous reports have indicated that ERs are intimately involved in the regulation of thymic tumor development and progression.[17-19] Therefore, it is important to examine the expression of GR and other steroid receptors in thymic tumors.

However, to the best of our knowledge, currently, the clinicopathological significance of GR, ER, and PgR expression in thymoma and thymic carcinoma is unknown. In the current study, we immunohistochemically analyzed the expression of GR, ERα, ERβ, PgR-A, and androgen receptor (AR) in thymic epithelial tumors (thymomas and thymic carcinomas). We also analyzed the correlation between the expression of these steroid receptors and clinical features. These data will serve as background information for studies assessing the predictive value of molecular markers of sensitivity to antihormone therapy.

MATERIALS AND METHODS

Patient Population

This study included 140 patients who underwent surgical resection for a thymic tumor at the National Cancer Center Hospital in Tokyo, Japan between 1973 and 2009 for thymic carcinoma and between 1999 and 2009 for thymoma (Table 1). An institutional review board approved this study.

All hematoxylin-and-eosin–stained slides, special stains, and the immunohistochemical analyses available were reviewed. Histologic diagnosis was based on the classification schema of the latest edition of the World Health Organization classification.[20]

Microarray Construction

The most representative tumor areas were sampled for the tissue microarray (TMA). The TMAs were assembled with a tissue-arraying instrument (Azumaya, Tokyo, Japan). To reduce sampling bias because of tumor heterogeneity, we used 2 replicate cores measuring 2.0 mm in diameter from different areas of individual tumors.

Immunohistochemical Analysis

For immunohistochemical staining, 4 μm-thick sections were routinely deparaffinized. The sections were exposed to 3% hydrogen peroxide for 15 minutes to block endogenous peroxidase activity and then washed in deionized water for 2 to 3 minutes. Heat-induced epitope retrieval was performed with citrate buffer solution (pH 6.0) (Muto Pure Chemicals Co., Tokyo, Japan) for GR and PgR-A or with Target Retrieval Solution (pH 9.0) (Dako Corporation, Carpinteria, Calif) for ERβ and AR. After the slides were allowed to cool at room temperature for approximately 30 minutes, they were rinsed with deionized water. The slides were then incubated with primary antibodies against GR (1:200, H8004; Perseus Proteomics, Tokyo, Japan), ERβ (1:100, EMR02; Leica, Wetzlar, Germany), PgR-A (1:400, 636; Dako Corporation), and AR (1:100, AR441; Dako Corporation) for 1 hour at room temperature. Immunoreactions were detected using the Envision-Plus system (Dako Corporation) and visualized with 3,3′-diaminobenzidine; counterstaining was performed with hematoxylin. Immunohistochemistry (IHC) for the ERα antibody (1:100, CONFIRM Estrogen Receptor SP1; Ventana, Tucson, Ariz) was processed by the BenchMark XT automated slide processing system (Ventana) according to the manufacturer's protocol.

IHC Scoring System

The IHC signal was evaluated using the Allred score, which assessed ERα status in breast carcinoma by IHC.[21] This system was used because it was easy to learn and highly reproducible.[21] Briefly, a proportion score was assigned, which represented the estimated proportion of positively staining tumor cells (0 indicates none; 1, $\leq$ 1/100; 2, 1/100 to $<$ 1/10; 3, 1/10 to $<$ 1/3; 4, 1/3 to $<$ 2/3; and 5, $\geq$ 2/3). An intensity score was assigned based on the average estimated intensity of staining in positive cells (0 indicates none; 1, weak intensity [immunoreactivity was only observed at $\times$ 100 magnification]; 2, intermediate intensity [immunoreactivity was detected at $\times$ 40 magnification but was weaker compared with positive controls]; and 3, strong intensity [immunoreactivity was easily detected at $\times$ 40 magnification]). The proportion score and intensity score were added to obtain a total score that ranged from 0 to 8. A total score of $\geq$ 3 was defined as positive for ERα, ERβ, PgR-A, and AR (Fig. 1). For GR, the Allred score was determined using 3 criteria (ie, total scores of $\geq$ 3, $\geq$ 4, and $\geq$ 5, to explore the best threshold).

Statistical Analysis

We analyzed thymomas and thymic carcinomas and categorized the former into 3 groups: type A + AB, type B1 + B2, and type B3 thymomas because although type A and AB and type B1 and B2 have similar clinical behaviors, type B3 differs from the other types of thymoma. In addition, we combined Masaoka stage into 2 groups for the analysis: stage I + II and stage III + IV according to the

Table 1. Patient Characteristics According to ERα, ERβ, PgR-A, AR, and GR IHC Score[a]

	All Patients	GR IHC			ERα IHC			ERβ IHC			PgR-A IHC			AR IHC		
Variable		Positive	Negative	*P*	Positive	Negative	*P*	Positive	Negative	*P*	Positive	Negative	*P*	Positive	Negative	*P*
Sex				.62			.15			.15			.20			.84
Male	53	45	8		10	43		44	9		1	52		13	40	
Female	87	71	16		9	78		63	24		0	87		20	67	
Age, y				.69			.67			.18			.36			.15
Median	57.4	58.0	54.9		57.1	57.5		59.0	52.2		67	57.4		56.3	57.8	
Range	25-84	25-84	32-74		25-79	28-84		25-84	28-76		67	25-84		25-79	28-84	
Histology (WHO)				.43			<.001			<.001			.47			.029
Type A +AB	57	47	10		2	55		54	3		0	57		14	43	
Type B1+B2	40	36	4		11	29		25	15		1	39		13	27	
Type B3	6	5	1		3	3		2	4		0	6		3	3	
Thymic carcinoma	37	28	9		3	34		26	11		0	37		3	34	
Masaoka stage				.17			.48			.008			.51			.21
I + II	98	84	14		12	86		81	17		1	97		26	72	
III + IV	42	32	10		7	35		26	16		0	42		7	35	
Tumor size, cm				.030			.021			.16			.37			.87
Median	6.01	6.03	5.92		6.24	5.97		5.79	6.72		8	6.01		6.16	5.97	
Range	1.5-13	1.5-13	1.5-9.0		1.5-13	1.5-12.5		1.5-12.5	3.5-13		8	1.5-13		1.5-12	1.5-13	

Abbreviations: AR, androgen receptor; ER, estrogen receptor; GR, glucocorticoid receptor; IHC, immunohistochemistry; PgR-A, progesterone receptor A; WHO, World Health Organization.
[a] Missing data were excluded from the analysis.

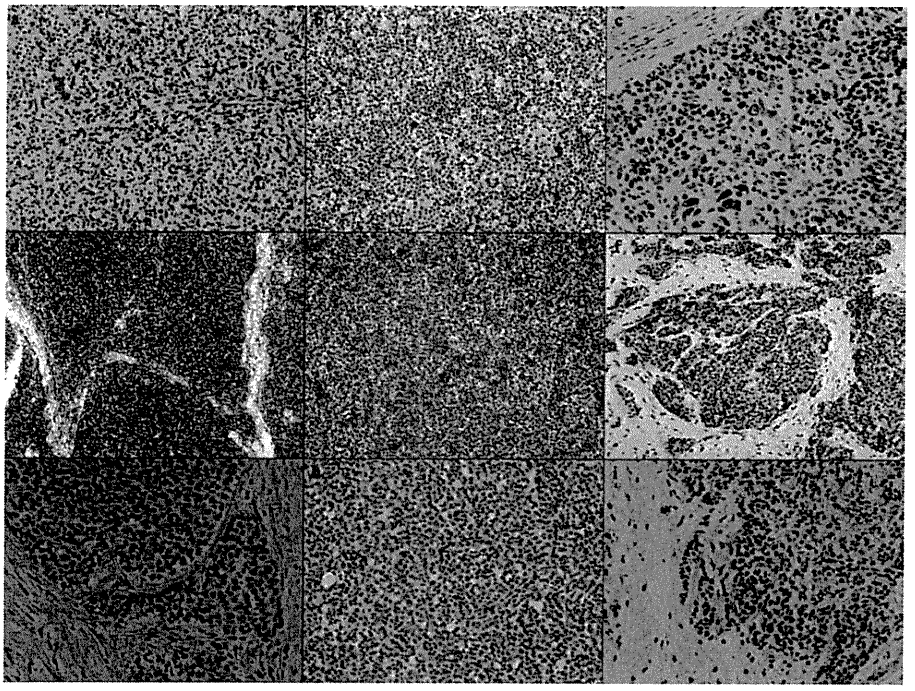

Figure 1. Representative images of positive immunohistochemical staining for glucocorticoid receptor (GR), estrogen receptor β (ERβ), and androgen receptor (AR) are shown. (a) GR expression in type A thymoma is shown (× 20). (b) GR expression in type B2 thymoma is shown (× 20). (c) GR expression in thymic carcinoma is shown (× 20). (d) ERβ expression in type A thymoma is shown (× 10). (e) ERβ expression in type B1 thymoma is shown (× 10). (f) ERβ expression in thymic carcinoma is shown (× 10). (g) AR expression in type AB thymoma is shown (× 20). (h) AR expression in type B2 thymoma is shown (× 20). (i) AR expression in thymic carcinoma is shown (× 20).

presence of invasion or metastasis to other organs. The Mann-Whitney *U* test for continuous variables and chi-square tests for categorical variables were used. A *P* value $\leq .05$ was regarded as statistically significant. Overall survival (OS) curves were calculated using the Kaplan-Meier method. Univariate survival analysis was performed with the log-rank test and Cox proportional hazards regression. Each variable was analyzed using the multivariate Cox model that was suitable for the variables with $P < .10$ from a Wald test of the univariate model. Statistical significance was set at $P \leq .05$.

RESULTS

Clinicopathologic Findings

A total of 140 cases of thymic epithelial tumors were studied, including 57 type A + AB, 40 type B1 + B2, and 6 type B3 thymomas and 37 thymic carcinomas. The patient cohort included 53 males and 87 females. The mean age of the patients at the time of diagnosis was 57.4 years (range, 25 years-84 years). Tumor size ranged from 1.5 cm to 13.0 cm (mean, 6.01 cm) (Table 1). The median follow-up was 64.6 months (range, 0.03 months-356.1 months). The 10-year survival rate in this patient cohort was 74.0% (95% confidence interval, 63.0%-85.0%), with 112 patients still alive at the time of last follow-up.

GR, ERα, ERβ, PgR-A, and AR Expression

Representative cases of positive expression of GR, ERβ, and AR for each histologic subtype are shown in Figure 1. For GR expression, we used 3 criteria: Allred scores of ≥ 3, ≥ 4, and ≥ 5. For any of the criteria, no significant differences were detected between GR expression and sex, age, histologic subtype, or tumor stage (data not shown). The difference between GR expression and tumor size was significant for total scores ≥ 5 and ≥ 4 ($P = .030$ and $P = .043$, respectively), but not for a total score ≥ 3 ($P = .110$). GR expression and OS were found to have a significant correlation only for a total score ≥ 5 ($P = .0125$). Thus, we adopted the total score ≥ 5 as being indicative of positive GR expression.

GR expression was detected in 116 (82.9%) patients, which included 47 (of 57 patients 82.5%)

Table 2. Coexpression Status for GR and ERβ, GR and AR, or ERβ and AR

	ERβ			AR		
	Positive	Negative	*P*	Positive	Negative	*P*
GR positive: TS ≥3			.75			.22
GR positive	102	31		30	103	
Negative	5	2		3	4	
GR positive: TS ≥4			.48			.48
GR positive	101	30		30	101	
Negative	6	3		3	6	
GR positive: TS ≥5			.22			.22
GR positive	91	25		25	91	
Negative	16	8		8	16	
AR positive: TS >3			.72			—
AR positive	26	7		—	—	
Negative	81	26		—	—	

Abbreviations: AR, androgen receptor; ER, estrogen receptor; GR, glucocorticoid receptor; TS, total score for Allred score.

patients with type A + AB thymoma, 36 (of 40 cases; 90%) with type B1 + B2 thymoma, 5 (of 6 cases; 83.3%) with type B3 thymoma, and 28 (of 37 cases; 75.7%) with thymic carcinoma ($P = .426$). No significant difference was recognized among the histologic subtypes.

ERα expression was detected in 19 (13.6%) patients, which included 2 (of 57 cases; 3.5%) patients with type A + AB thymoma, 11 (of 40 cases; 27.5%) with type B1 + B2 thymoma, 3 (of 6 cases; 50%) with type B3 thymoma, and 3 (of 37 cases; 8.1%) with thymic carcinoma ($P < .001$). Significant differences were detected between type A + AB thymoma and other histological subtypes; type B1 + B2 thymoma ($P = .002$), type B3 thymoma ($P = .006$), and thymic carcinoma ($P = .046$); and type B3 thymoma and thymic carcinoma ($P = .019$).

ERβ expression was detected in 107 (76.4%) patients, which included 54 (of 57 cases; 94.7%) patients with type A + AB thymoma, 25 (of 40 cases; 62.5%) with type B1 + B2 thymoma, 2 (of 6 cases; 33.3%) with type B3 thymoma, and 26 (of 37 cases; 70.3%) with thymic carcinoma ($P < .001$). Significant differences were detected between type A + AB and type B1 + B2 thymoma ($P = .001$), type B3 thymoma ($P = .002$), and thymic carcinoma ($P = .021$).

PgR-A expression was detected in only 1 (0.71%) patient. The thymoma was type B1 + B2 (1 of 46 cases; 2.2%). No significant difference was observed compared with the other histologic subtypes.

AR expression was detected in 33 (23.6%) patients, which included 14 (of 57 cases; 24.6%) patients with type A + AB thymoma, 13 (of 40 cases; 32.5%) with type B1 + B2 thymoma, 3 (of 6 cases; 50%) with type B3 thymoma, and 3 (of 37 cases; 8.1%) with thymic carcinoma ($P = .029$). A marginal difference was detected between type B1 + B2 thymoma and thymic carcinoma ($P = .054$).

With regard to coexpression status, no significant differences were detected among the subtypes (Table 2).

In the association analysis between clinicopathologic factors and hormone receptor expression, significant correlations were observed between ERα expression and tumor size ($P = .021$) and between ERβ expression and tumor stage ($P = .008$). The other clinicopathologic factors demonstrated no statistically significant correlation with the expression status of any of the hormone receptors (Table 1). In addition, no significant differences were detected in the expression levels of GR, ERβ, and AR between type A and type AB thymomas or between type B1 and type B2 thymomas (data not shown).

Correlation of OS With Clinicopathologic Factors and Steroid Receptor Expression

We investigated whether there was a correlation between OS and clinicopathologic factors or hormone receptor expression (Fig. 2). The 10-year OS rates for patients with type A + AB, type B1 + B2, and type B3 thymomas and thymic carcinoma were 92.6%, 89.5%, 75.0%, and 42.5%, respectively (thymoma vs thymic carcinoma; $P < .0001$) (Fig. 2a). Significant differences were found between thymic carcinoma and type A + AB thymoma and between thymic carcinoma and type B1 + B2

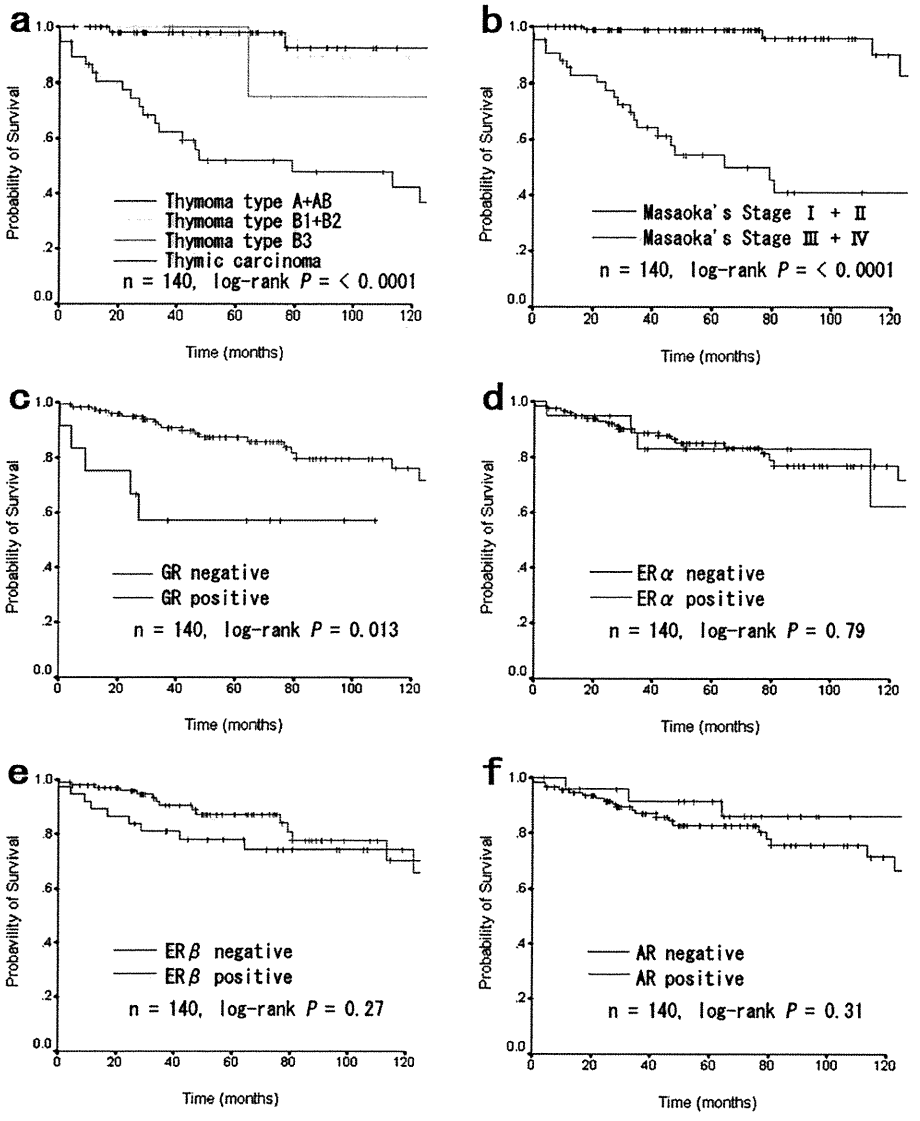

Figure 2. (a) Overall survival (OS) is shown according to histologic subtype (ie, type A + AB thymoma, type B1 + B2 thymoma, type B3 thymoma, and thymic carcinoma). (b) OS is shown according to Masaoka stage (ie, stage I + II and stage III + IV). (c) OS is shown according to glucocorticoid receptor (GR) immunohistochemistry (IHC) score (positive indicates a total score ≥ 5; negative, total score ≤ 4). (d) OS is shown according to estrogen receptor α (ERα) IHC score (positive indicates a total score ≥ 3; negative, total score ≤ 2). (e) OS is shown according to ERβ IHC score (positive indicates a total score ≥ 3; negative, total score ≤ 2). (f) OS is shown according to androgen receptor (AR) IHC score (positive indicates a total score ≥ 3; negative, total score ≤ 2).

thymoma (both $P < .0001$), whereas no significant difference between thymic carcinoma and type B3 thymoma was detected ($P = .15$). In addition, no significant difference was detected between type B1 + B2 and type B3 thymomas with regard to the 10-year OS rates ($P = .30$) (data not shown). The 10-year OS rates for Masaoka stage I + II and stage III + IV were 82.5% and 41.0%, respectively ($P < .0001$) (Fig. 2c). With regard to negative and positive hormone receptor status (Figs. 2c-2f), the 10-year OS rates for GR were 65.7% and 75.6%, respectively ($P = .013$); 76.8% and 62.2%, respectively, for ERα ($P = .79$); 74.3% and 71.9%, respectively, for ERβ ($P = .27$); and 71.1% and 85.0%, respectively, for AR ($P = .31$).

Multivariate analysis revealed that histologic subtype ($P = .0039$), tumor stage ($P = .0012$), and GR expression ($P = .0025$) were significantly correlated with the 10-year OS, whereas no significant correlation was detected between the other variables and OS (Table 3).

Table 3. Univariate, Multivariate, and Bootstrap Analysis of Survival

	Univariate Analysis			Multivariate Analysis		
Variable	HR	95% CI	*P*	HR	95% CI	*P*
Histology (WHO)						
Thymoma vs thymic carcinoma	11.6	4.3-31.3	<.0001	5.69	1.8-18.5	.0039
Masaoka stage						
I + II vs III + IV	14.9	5.1-43.2	<.0001	2.66	1.5-4.8	.0012
Sex						
Male vs female	0.81	0.38-1.7	.59	—	—	—
Age, y						
Continuous	1.0	0.97-1.0	.94	—	—	—
Tumor size, cm						
Continuous	1.1	0.89-1.2	.58	—	—	—
GR protein expression						
Negative vs positive	0.35	0.15-0.83	.013	0.24	0.10-0.61	.0025
ERα protein expression						
Negative vs positive	1.2	0.40-3.4	.79	—	—	—
ERβ protein expression						
Negative vs positive	0.64	0.29-1.4	.27	—	—	—
AR protein expression						
Negative vs positive	0.58	0.20-1.7	.31	—	—	—

Abbreviations: 95% CI, 95% confidence interval; AR, androgen receptor; ER, estrogen receptor; GR, glucocorticoid receptor; HR, hazard ratio; WHO, World Health Organization.

DISCUSSION

In the current study, high rates of GR and ERβ expression were observed in thymoma and thymic carcinoma. Furthermore, multivariate analysis revealed that GR expression was associated with better prognosis in those patients with surgically resected thymoma and thymic carcinoma. In addition, we established possible criteria for GR expression in IHC.

To our knowledge, the underlying mechanism of the better prognosis noted for patients with GR protein-expressing tumors, including thymic epithelial tumors, remains unknown. However, it has been shown that GCs contribute in eliciting a positive clinical response in patients with pediatric acute lymphoblastic leukemia or metastatic prostate cancer.[22,23] Moreover, some studies have reported that the administration of GC demonstrated a dramatic response among patients with thymic epithelial tumors, indicating that GC acts a tumor suppressor through the GR in thymic epithelial tumors.[7-13] There have been conflicting results concerning the antitumor effects of GCs. In some tumors, GCs assist tumor progression by inhibiting chemotherapy-induced or immunoresponse-induced apoptosis, promoting tumor growth[24] and increasing cancer invasiveness.[25-27] Conversely, GC induces tumor apoptosis by negatively affecting the transcription of nuclear factor kappaB (*NF-κB*), an important regulator of the immune system and antiapoptotic mechanisms, in various cell lines and lymphocytes.[28-30] In vitro analysis revealed that GCs induce cell cycle arrest and apoptosis in epithelial cells of thymic neoplasms.[4]

Similar to the results of the current study, some tumors that express GR in other organs have shown favorable outcomes and a statistically significant correlation with OS.[31,32] In the correlation analysis of the current study between GR expression score and clinicopathologic factors, the patients with a higher GR expression score demonstrated a more favorable outcome. This result suggested that a low level of physiologic GCs may exert antineoplastic effects. The possible effects of physiologic sex steroids have been demonstrated in the progression of breast and prostate cancers.[33-37] Physiologic steroid hormones can also affect systemic organs. Thus, the results of the current study indicate that physiologic GCs may also play a role in the inhibition of tumorigenesis of thymic epithelial tumors.

The observed immunohistochemical positivity of ERα was low (19 cases; 13.6%) compared with a previous report in which approximately two-thirds of thymoma

cases were positive.[38] One possible reason for this discrepancy is that because ERα expression was heterogeneously distributed, areas with positive ERα expression could not be easily detected on TMA, which was a tiny area compared with the whole section. Another possible reason is the differences in the specificity and sensitivity of the antibodies used for ERα. The clone 6F11 that was used in the previous study was not highly specific for ERα. Clone 6F11 recognizes the full-length protein. Because the full-length ERβ protein is homologous to the full-length ERα protein, clone 6F11 may recognize ERβ as ERα, with particular binding in the DNA binding domain . Furthermore, we used a highly sensitive rabbit monoclonal antibody (clone SP1) that demonstrated an 8-fold higher affinity than the mouse antibody.[39] Thus, the results of the current study indicate that the immunohistochemical positivity of ERα is not very high in both thymoma and thymic carcinoma.

Unlike ERα expression, we detected high expression of the ERβ protein (76.4%). In addition, the results of the current study demonstrated a high positivity (94.7%) in type A + AB thymoma and a decreased positivity (33.3%) in type B3 thymoma. This result indicates that the high expression of ERα noted in the earlier mentioned study may be because of a cross-reaction with ERβ. To the best of our knowledge, there was only 1 report published to date analyzing ERβ expression in thymomas, and the expression rate was extremely low (7%)[38] compared with that observed in the current study. This discrepancy may be because of differences in the patient population, source of antibody, dilution, method of antigen retrieval, and scoring system. Among these, the most likely factor was the difference in the source of antibody. The clone EMR02, which was used in the current study, recognizes the C-terminus, whereas the clone 06-629 that was used in the previous study recognizes the N-terminus. Another possibility was the difference in the patient population.

The issue of whether ERβ is a target in tumor therapy is controversial. However, there is increasing evidence in several studies that ERβ is significantly related to cancer invasiveness. ERβ expression has been frequently observed in metastases of prostate cancer using IHC.[40] In addition, in vivo and in vitro studies have demonstrated that ERβ exerts stimulative effects on breast cancer development and metastasis.[41] It has also been shown that ERβ negatively affects malignant cell tumorigenesis.[19,42,43] Although to our knowledge the exact correlation between ERβ expression and tumor progression in thymic epithelial tumors is still unclear, ERβ is suggested as a potential target in the treatment of ERβ-positive thymomas and thymic carcinomas.

In the current study, we found that PgR-A and AR proteins were expressed at low levels in thymomas and thymic carcinomas. The previous study also demonstrated low expression rates of PgR-A (4%) and AR (15%).[38] These results indicate that PgR-A and AR have low potential as targets for therapy and have little involvement in thymoma and thymic tumorigenesis.

The results of the current study also demonstrated a significant correlation of histologic subtype and tumor stage with OS. There have been conflicting results concerning prognosis among the histologic subtypes of thymic epithelial tumors.[44-49] Some reports have shown that patients with type B3 thymoma have a worse prognosis than those with type B2 thymoma,[44,45] whereas others have reported no significant difference in survival between these 2 groups.[46-49] The results of the current study indicated no difference in the 10-year OS rates between patients with type B1 + B2 (89.5%) and type B3 (75.0%) thymomas ($P = .30$), whereas significant differences ($P < .001$) were noted between patients with type B1 + B2 (86% and 85%, respectively) and type B3 (38%) thymomas in a previous report from our institution.[44] A possible reason is the difference in the period of analysis; the analysis of the current study was conducted between 1999 and 2009 for thymoma, whereas that of the previous report was performed between 1962 and 2000.

The results of the current study demonstrated a high rate of GR and ERβ expression in thymomas and thymic carcinomas. Furthermore, multivariate analysis revealed that GR expression was associated with better prognosis in patients with surgically resected thymomas and thymic carcinomas. These associations should be validated through prospective studies that include greater numbers of cases.

FUNDING SOURCES

No specific funding was disclosed.

CONFLICT OF INTEREST DISCLOSURES

The authors made no disclosures.

REFERENCES

1. Cole TJ, Blendy JA, Monaghan AP, et al. Targeted disruption of the glucocorticoid receptor gene blocks adrenergic chromaffin cell development and severely retards lung maturation. *Genes Dev.* 1995;9:1608-1621.

2. Rhen T, Cidlowski JA. Antiinflammatory action of glucocorticoids–new mechanisms for old drugs. *N Engl J Med.* 2005;353:1711-1723.
3. Yamamoto KR. Steroid receptor regulated transcription of specific genes and gene networks. *Annu Rev Genet.* 1985;19:209-252.
4. Funakoshi Y, Shiono H, Inoue M, et al. Glucocorticoids induce G1 cell cycle arrest in human neoplastic thymic epithelial cells. *J Cancer Res Clin Oncol.* 2005;131:314-322.
5. Oakley RH, Webster JC, Sar M, Parker CR Jr, Cidlowski JA. Expression and subcellular distribution of the beta-isoform of the human glucocorticoid receptor. *Endocrinology.* 1997;138:5028-5038.
6. Wyllie AH. Glucocorticoid-induced thymocyte apoptosis is associated with endogenous endonuclease activation. *Nature.* 1980;284:555-556.
7. Hu E, Levine J. Chemotherapy of malignant thymoma. Case report and review of the literature. *Cancer.* 1986; 57:1101-1104.
8. Kobayashi Y, Fujii Y, Yano M, et al. Preoperative steroid pulse therapy for invasive thymoma: clinical experience and mechanism of action. *Cancer.* 2006;106:1901-1907.
9. Kodama K, Doi O, Higashiyama M, Yokouchi H, Yasuda T, Funai H. Dramatic response of postthymomectomy myasthenia gravis with multiple lung nodules to corticosteroids. *Ann Thorac Surg.* 1997;64:555-557.
10. Loehrer PJ Sr, Wang W, Johnson DH, Aisner SC, Ettinger DS. Octreotide alone or with prednisone in patients with advanced thymoma and thymic carcinoma: an Eastern Cooperative Oncology Group Phase II Trial. *J Clin Oncol.* 2004;22:293-299.
11. Palmieri G, Lastoria S, Colao A, et al. Successful treatment of a patient with a thymoma and pure red-cell aplasia with octreotide and prednisone. *N Engl J Med.* 1997;336:263-265.
12. Tiseo M, Monetti F, Ferrarini M, Serrano J, Chiaramondia M, Ardizzoni A. CASE 1. Complete remission to corticosteroids in an octreotide-refractory thymoma. *J Clin Oncol.* 2005;23:1578-1579.
13. Palmieri G, Montella L, Martignetti A, et al. Somatostatin analogs and prednisone in advanced refractory thymic tumors. *Cancer.* 2002;94:1414-1420.
14. Alexieva-Figusch J, Van Putten WL, Blankenstein MA, Blonk-Van Der Wijst J, Klijn JG. The prognostic value and relationships of patient characteristics, estrogen and progestin receptors, and site of relapse in primary breast cancer. *Cancer.* 1988;61:758-768.
15. Nilsson B, Bergqvist A, Lindblom D, Ljungberg O, Sodergard R, von Schoultz B. Characterization and localization of specific oestrogen binding in the human thymus. *Gynecol Obstet Invest.* 1986;21:150-157.
16. Nilsson B, Ferno M, von Schoultz B. Estrogen and progesterone receptors in the human thymus. *Gynecol Obstet Invest.* 1990;29:289-291.
17. Gong H, Jarzynka MJ, Cole TJ, et al. Glucocorticoids antagonize estrogens by glucocorticoid receptor-mediated activation of estrogen sulfotransferase. *Cancer Res.* 2008; 68:7386-7393.
18. Ishibashi H, Suzuki T, Suzuki S, et al. Estrogen inhibits cell proliferation through in situ production in human thymoma. *Clin Cancer Res.* 2005;11:6495-6504.
19. Pinton G, Brunelli E, Murer B, et al. Estrogen receptor-beta affects the prognosis of human malignant mesothelioma. *Cancer Res.* 2009;69:4598-4604.
20. Travis WD, Brambilla E, Muller-Hermelink HK, Harris CC. Pathology and genetics tumors of the lung, pleura, thymus and heart. In: World Health Organization Classification of Tumours. Lyon, France: IARC Press; 2004:145-248.
21. Allred DC, Harvey JM, Berardo M, Clark GM. Prognostic and predictive factors in breast cancer by immunohistochemical analysis. *Mod Pathol.* 1998;11:155-168.
22. Pui CH, Evans WE. Treatment of acute lymphoblastic leukemia. *N Engl J Med.* 2006;354:166-178.
23. Storlie JA, Buckner JC, Wiseman GA, Burch PA, Hartmann LC, Richardson RL. Prostate specific antigen levels and clinical response to low dose dexamethasone for hormone-refractory metastatic prostate carcinoma. *Cancer.* 1995;76: 96-100.
24. Zhang C, Beckermann B, Kallifatidis G, et al. Corticosteroids induce chemotherapy resistance in the majority of tumour cells from bone, brain, breast, cervix, melanoma and neuroblastoma. *Int J Oncol.* 2006;29:1295-1301.
25. Filderman AE, Bruckner A, Kacinski BM, Deng N, Remold HG. Macrophage colony-stimulating factor (CSF-1) enhances invasiveness in CSF-1 receptor-positive carcinoma cell lines. *Cancer Res.* 1992;52:3661-3666.
26. Rutz HP, Herr I. Interference of glucocorticoids with apoptosis signaling and host-tumor interactions. *Cancer Biol Ther.* 2004;3:715-718.
27. Sapi E, Flick MB, Gilmore-Hebert M, Rodov S, Kacinski BM. Transcriptional regulation of the c-fms (CSF-1R) proto-oncogene in human breast carcinoma cells by glucocorticoids. *Oncogene.* 1995;10:529-542.
28. Auphan N, DiDonato JA, Rosette C, Helmberg A, Karin M. Immunosuppression by glucocorticoids: inhibition of NF-kappa B activity through induction of I kappa B synthesis. *Science.* 1995;270:286-290.
29. Scheinman RI, Cogswell PC, Lofquist AK, Baldwin AS Jr. Role of transcriptional activation of I kappa B alpha in mediation of immunosuppression by glucocorticoids. *Science.* 1995;270:283-286.
30. Wang CY, Mayo MW, Korneluk RG, Goeddel DV, Baldwin AS Jr. NF-kappaB antiapoptosis: induction of TRAF1 and TRAF2 and c-IAP1 and c-IAP2 to suppress caspase-8 activation. *Science.* 1998;281:1680-1683.
31. Kato GJ, Quddus FF, Shuster JJ, et al. High glucocorticoid receptor content of leukemic blasts is a favorable prognostic factor in childhood acute lymphoblastic leukemia. *Blood.* 1993;82:2304-2309.
32. Lu YS, Lien HC, Yeh PY, et al. Glucocorticoid receptor expression in advanced non-small cell lung cancer: clinicopathological correlation and in vitro effect of glucocorticoid on cell growth and chemosensitivity. *Lung Cancer.* 2006;53: 303-310.
33. Yao K, Lee ES, Bentrem DJ, et al. Antitumor action of physiological estradiol on tamoxifen-stimulated breast tumors grown in athymic mice. *Clin Cancer Res.* 2000;6: 2028-2036.
34. Gottardis MM, Jordan VC. Development of tamoxifen-stimulated growth of MCF-7 tumors in athymic mice after long-term antiestrogen administration. *Cancer Res.* 1988;48: 5183-5187.
35. Ozasa K, Nakao M, Watanabe Y, et al. Serum phytoestrogens and prostate cancer risk in a nested case-control study among Japanese men. *Cancer Sci.* 2004;95:65-71.
36. Travis RC, Key TJ, Allen NE, et al. Serum androgens and prostate cancer among 643 cases and 643 controls in the

European Prospective Investigation into Cancer and Nutrition. *Int J Cancer.* 2007;121:1331-1338.
37. Gann PH, Hennekens CH, Ma J, Longcope C, Stampfer MJ. Prospective study of sex hormone levels and risk of prostate cancer. *J Natl Cancer Inst.* 1996;88:1118-1126.
38. Ishibashi H, Suzuki T, Suzuki S, et al. Sex steroid hormone receptors in human thymoma. *J Clin Endocrinol Metab.* 2003;88:2309-2317.
39. Huang Z, Zhu W, Szekeres G, Xia H. Development of new rabbit monoclonal antibody to estrogen receptor: immunohistochemical assessment on formalin-fixed, paraffin-embedded tissue sections. *Appl Immunohistochem Mol Morphol.* 2005;13:91-95.
40. Lai JS, Brown LG, True LD, et al. Metastases of prostate cancer express estrogen receptor-beta. *Urology.* 2004;64:814-820.
41. Hou YF, Yuan ST, Li HC, et al. ERbeta exerts multiple stimulative effects on human breast carcinoma cells. *Oncogene.* 2004;23:5799-5806.
42. Hartman J, Strom A, Gustafsson JA. Estrogen receptor beta in breast cancer–diagnostic and therapeutic implications. *Steroids.* 2009;74:635-641.
43. Guerini V, Sau D, Scaccianoce E, et al. The androgen derivative 5alpha-androstane-3beta,17beta-diol inhibits prostate cancer cell migration through activation of the estrogen receptor beta subtype. *Cancer Res.* 2005;65:5445-5453.
44. Nakagawa K, Asamura H, Matsuno Y, et al. Thymoma: a clinicopathologic study based on the new World Health Organization classification. *J Thorac Cardiovasc Surg.* 2003; 126:1134-1140.
45. Okumura M, Ohta M, Tateyama H, et al. The World Health Organization histologic classification system reflects the oncologic behavior of thymoma: a clinical study of 273 patients. *Cancer.* 2002;94:624-632.
46. Chalabreysse L, Roy P, Cordier JF, Loire R, Gamondes JP, Thivolet-Bejui F. Correlation of the WHO schema for the classification of thymic epithelial neoplasms with prognosis: a retrospective study of 90 tumors. *Am J Surg Pathol.* 2002;26:1605-1611.
47. Chen G, Marx A, Wen-Hu C, et al. New WHO histologic classification predicts prognosis of thymic epithelial tumors: a clinicopathologic study of 200 thymoma cases from China. *Cancer.* 2002;95:420-429.
48. Rieker RJ, Hoegel J, Morresi-Hauf A, et al. Histologic classification of thymic epithelial tumors: comparison of established classification schemes. *Int J Cancer.* 2002;98: 900-906.
49. Strobel P, Bauer A, Puppe B, et al. Tumor recurrence and survival in patients treated for thymomas and thymic squamous cell carcinomas: a retrospective analysis. *J Clin Oncol.* 2004;22:1501-1509.

Multicenter analysis of high-resolution computed tomography and positron emission tomography/computed tomography findings to choose therapeutic strategies for clinical stage IA lung adenocarcinoma

Morihito Okada, MD, PhD,[a] Haruhiko Nakayama, MD, PhD,[b] Sakae Okumura, MD, PhD,[c] Hiromitsu Daisaki, PhD,[d] Shuji Adachi, MD, PhD,[e] Masahiro Yoshimura, MD, PhD,[f] and Yoshihiro Miyata, MD, PhD[a]

Objective: The detection rates of small lung cancers, especially adenocarcinoma, have recently increased. An understanding of malignant aggressiveness is critical for the selection of suitable therapeutic strategies, such as sublobar resection. The objective of this study was to examine the malignant biological behavior of clinical stage IA adenocarcinoma and to select therapeutic strategies using high-resolution computed tomography, fluorodeoxyglucose-positron emission tomography/computed tomography, and a pathologic analysis in the setting of a multicenter study.

Methods: We performed high-resolution computed tomography and fluorodeoxyglucose-positron emission tomography/computed tomography in 502 patients with clinical T1N0M0 adenocarcinoma before they underwent surgery with curative intent. We evaluated the relationships between clinicopathologic characteristics and maximum standardized uptake values on fluorodeoxyglucose-positron emission tomography/computed tomography, ground-glass opacity ratio, and tumor disappearance rate on high-resolution computed tomography and component of bronchioloalveolar carcinoma on surgical specimens, as well as between these and surgical findings. We used a phantom study to correct the serious limitation of any multi-institution study using positron emission tomography/computed tomography, namely, a discrepancy in maximum standardized uptake values among institutions.

Results: Analyses of receiver operating characteristic curves identified an optimal cutoff value to predict high-grade malignancy of 2.5 for revised maximum standardized uptake values, 20% for ground-glass opacity ratio, 30% for tumor disappearance rate, and 30% for bronchioloalveolar carcinoma ratio. Maximum standardized uptake values and bronchioloalveolar carcinoma ratio, tumor disappearance rate, and ground-glass opacity ratio mirrored the pathologic aggressiveness of tumor malignancy, nodal metastasis, recurrence, and prognosis, including disease-free and overall survival.

Conclusions: Maximum standardized uptake value is a significant preoperative predictor for surgical outcomes. High-resolution computed tomography and fluorodeoxyglucose-positron emission tomography/computed tomography findings are important to determine the appropriateness of sublobar resection for treating clinical stage IA adenocarcinoma of the lung. (J Thorac Cardiovasc Surg 2011;141:1384-91)

From the Department of Surgical Oncology,[a] Hiroshima University, Hiroshima, Japan; Department of Thoracic Surgery,[b] Kanagawa Cancer Center, Yokohama, Japan; Department of Thoracic Surgery,[c] Cancer Institute Hospital, Tokyo, Japan; Department of Radiology,[d] National Cancer Center, Tokyo, Japan; and Department of Radiology[e] and Thoracic Surgery,[f] Hyogo Cancer Center, Akashi, Japan.

Disclosures: Authors have nothing to disclose with regard to commercial support.
Received for publication Nov 26, 2010; revisions received Jan 21, 2011; accepted for publication Feb 9, 2011; available ahead of print March 28, 2011.

Address for reprints: Morihito Okada, MD, PhD, Department of Surgical Oncology, Research Institute for Radiation Biology and Medicine, Hiroshima University, 1-2-3-Kasumi, Minami-ku, Hiroshima City, Hiroshima 734-0037, Japan (E-mail: morihito@hiroshima-u.ac.jp).

0022-5223/$36.00

doi:10.1016/j.jtcvs.2011.02.007

The standard treatment for operable non–small cell lung cancer, even early clinical T1N0M0 disease, remains lobectomy with dissection of the hilar and mediastinal lymph nodes.[1] However, clinical investigations to date have demonstrated that sublobar resection, which chiefly consists of radical segmentectomy with nodal dissection, might be feasible for treating early lung cancers with the tangible advantages of maintained lung function and a reasonable prognosis.[2,3] To date, there are no means to preoperatively identify early lung cancers that are biologically less aggressive and may be better suited for a sublobar resection.

Recent advances in high-resolution computed tomography (HRCT) and the widespread application of computed tomography (CT) screening have enhanced the discovery of small lung cancers, particularly adenocarcinoma.[2,3] These early-stage cancers are biologically heterogeneous, and the malignant aggressiveness is not well characterized

Abbreviations and Acronyms

AUC = area under the curve
BAC = bronchioloalveolar carcinoma
CT = computed tomography
DFS = disease-free survival
FDG = F-18 fluorodeoxyglucose
FOV = field of view
GGO = ground-glass opacity
HRCT = high-resolution computed tomography
maxSUV = maximum standardized uptake value
PET = positron emission tomography
ROC = receiver operating characteristic
SUV = standardized uptake value
TDR = tumor disappearance rate

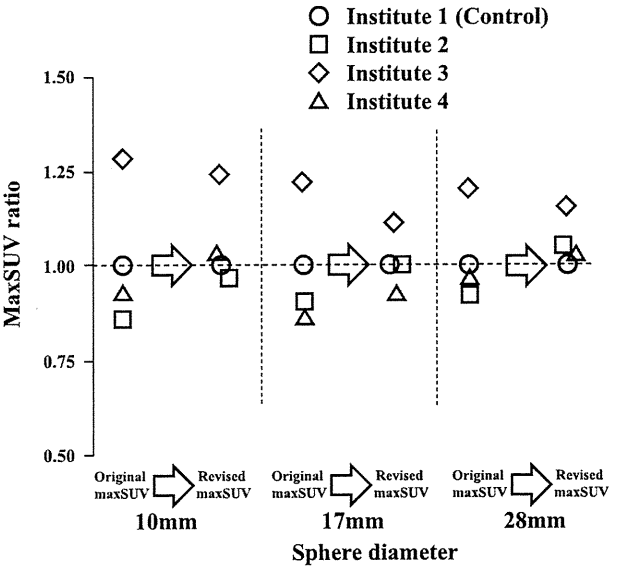

FIGURE 1. maxSUV adjusted using experimental phantom (revised maxSUV). Original maxSUV data were calibrated by multiplying calibration factors based on phantom studies to correct inter-institutional SUV variability. MaxSUV ratio is expressed as maxSUV of each institute for maxSUV of control institute (Institute 1). *maxSUV,* Maximum standardized uptake value.

at the time of diagnosis. This information should be considered in selecting the therapeutic strategy.

Positron emission tomography (PET)/CT with F-18 fluorodeoxyglucose (FDG) has become an integral part of the non–small cell lung cancer evaluation.[4-6] This modality generates quantitative images based on glucose metabolism reflecting the metabolic activity and proliferative potential of malignant tumors, and providing anatomic CT images. Small-scale studies have demonstrated the role of FDG-PET/CT in assessing the biological status of cancers,[7,8] but this requires confirmation in a larger cohort. Therefore, assessed the biological nature of small adenocarcinomas in more than 500 patients by using HRCT and FDG-PET/CT and the pathologic findings of surgical specimens in a multicenter setting. Because of the heterogeneity of PET techniques and performance, we corrected inter-institutional errors in maximum standardized uptake values (maxSUVs) resulting from PET/CT scanners of variable quality based on outcomes of a study using an anthropomorphic body phantom that conformed to National Electrical Manufacturers Association standards.[9]

PATIENTS AND METHODS

We enrolled 502 patients (female, 279 [56%]; male, 223 [44%]; mean age, 65.3 ± 9.6 years) with clinical T1N0M0 stage IA adenocarcinoma of the lung at 4 institutions between August 1, 2005, and December 31, 2009. All patients underwent HRCT and FDG-PET/CT followed by curative R0 resection. The ethics committees at each institution approved this multicenter study and the prospective database used in the analysis.

High-Resolution Computed Tomography

Chest images were obtained using 16-row multidetector CT independently of subsequent PET/CT examinations. High-resolution images of the tumors were acquired using the following parameters: 120 kVp, 200 mA, 1- to 2-mm section thickness, 512 × 512 pixel resolution, 0.5- to 1-second scanning time, a high spatial reconstruction algorithm with a 20-cm field of view (FOV) and mediastinal (level, 40 HU; width, 400 HU) and lung (level, –600 HU; width, 1600 HU) window settings. Ground-glass opacity (GGO) was defined as a misty increase in lung attenuation without obscuring the underlying vascular markings, and we defined the GGO ratio (%) as [1– (maximum dimension of consolidation of lung windows/maximum dimension of tumor of lung windows)] × 100. Tumor disappearance rate (TDR) (%) was defined as [1– (tumor area of the mediastinal windows/tumor area of the lung windows)] × 100.[2,3,10]

Fluorodeoxyglucose-Positron Emission Tomography/Computed Tomography

The patients fasted for more than 4 hours before being intravenously injected with 74-370 MBq of FDG, and then relaxed for at least 1 hour before FDG-PET/CT scanning. Blood glucose was calculated before tracer injection to confirm a level of less than 150 mg/dL.[11] Patients with blood glucose values of 150 mg/dL or greater were excluded from PET/CT acquisition. Images were obtained in this study using Discovery ST (GE Healthcare, Buckinghamshire, England), Aquiduo (Toshiba Medical Systems Corporation, Tochigi, Japan), or Biograph Sensation16 (Siemens Healthcare, South Iselin, NJ) integrated PET/CT scanners. Low-dose unenhanced CT images of a 2- to 4-mm section thickness for attenuation correction and localization of lesions identified by PET were obtained from the head to the pelvic floor of each patient using a standard protocol. Immediately after CT, PET covered the identical axial FOV for 2 to 4 minutes per table position depending on the condition of the patient and scanner performance. All PET images with a 50-cm FOV were reconstructed using an iterative algorithm with CT-derived attenuation correction. Variations in standardized uptake value (SUV) among institutions were minimized using the anthropomorphic body phantom. A calibration factor was analyzed by dividing the actual SUV by the gauged mean SUV in the phantom background to decrease inter-institutional SUV inconsistencies, and the final maxSUV used in this is referred to as revised maxSUV. The adjustment of the inter-institutional variability in SUV narrowed the range from 0.89 to 1.24 to 0.97 to 1.18 when maxSUV ratio was expressed as the maxSUV of each institute for the maxSUV of the control institute (Figure 1).

GTS

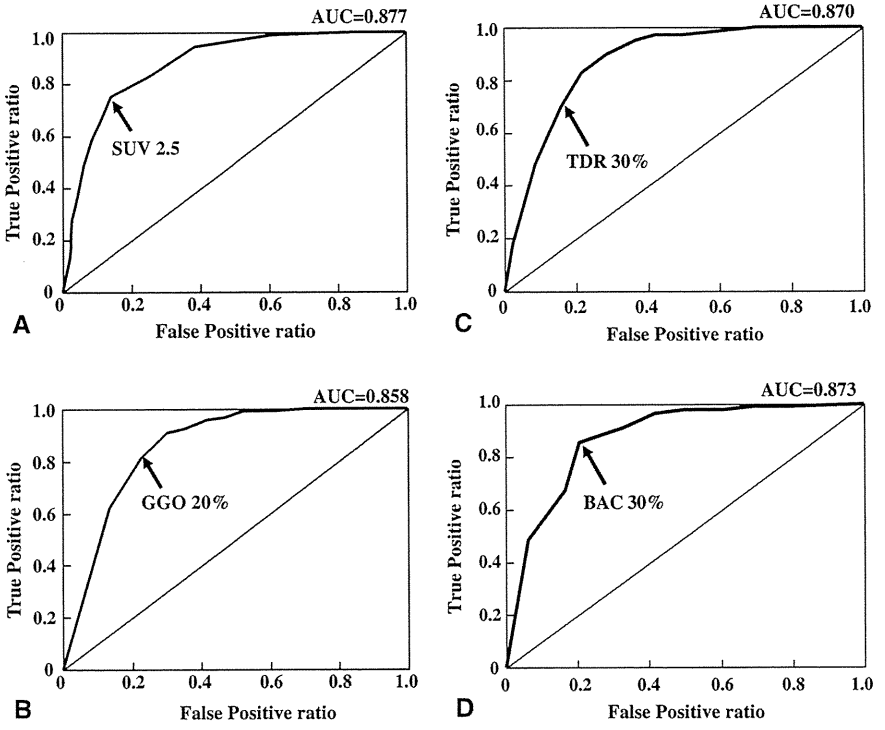

FIGURE 2. ROC curves for positive predictive values of pathologic lymph node metastasis, lymphatic invasion, blood vessel invasion, or pleural invasion. ROC curves are for revised maxSUV (A), GGO ratio (B), TDR (C), and BAC ratio (D). *maxSUV,* Maximum standardized uptake value; *GGO,* ground-glass opacity; *TDR,* tumor disappearance rate; *BAC,* bronchioloalveolar carcinoma; *AUC,* area under the curve; *SUV,* standardized uptake value.

Resected tumors were fixed in 10% formalin, embedded in paraffin, and pathologically evaluated (including the largest cut) using hematoxylin–eosin and Elastica van Gieson staining. The amount of bronchioloalveolar carcinoma (BAC) areas proportionate to whole tumors was approximately calculated as the BAC ratio. Independent observers and pathologists blindly evaluated GGO and BAC ratios and TDR, and corrected discrepancies among evaluations using mean values.

Receiver operating characteristic (ROC) curves of the revised maxSUV, GGO ratios, TDR, and BAC ratios to predict lymphatic, blood vessel, and pleural invasion or nodal involvement were generated to determine the cutoff values that yielded optimal sensitivity and specificity. The patient population was subdivided on the basis of the cutoff values of the revised SUVmax, GGO, TDR, and BAC ratios derived from ROC curves. We performed multiple logistic regression analyses to demonstrate independent variables of maxSUV, GGO ratio, TDR, and BAC ratio relative to the prediction of pathologic findings for high malignant grade and recurrence. Survival was calculated using the Kaplan–Meier method, and differences were determined using the log-rank test. Disease-free survival (DFS) was defined as time from date of surgery until the first event (relapse or death from any cause) or last follow-up. Overall survival was defined as time from the date of surgery until death from any cause or last follow-up.

RESULTS

The primary tumor measured by HRCT was 20 mm or less in diameter in 290 patients (58%) and 21 to 30 mm in 212 patients (42%). Lymphatic permeation, blood vessel, and pleural invasion was evident in 76 patients (15%), 92 patients (18%), and 56 patients (11%), respectively, and lymph nodes were involved in 38 (8%) of them.

The ROC curves identified optimal revised maxSUV, GGO, TDR, and BAC ratio cutoff values of 2.5 (area under the curve [AUC], 0.877), 20% (AUC, 0.858), 30% (AUC, 0.870), and 30% (AUC, 0.873), respectively, for predicting pathologic findings of high malignancy (Figure 2). At a cutoff value of 2.5, a high revised maxSUV significantly correlated with male gender, a high CEA value, large tumor, lymphatic invasion, vascular invasion, pleural invasion, and lymph node metastasis (Table 1). Likewise, low TDR, GGO, and BAC ratios were significantly associated with a high CEA value, lymphatic, vascular, pleural invasion, and lymph node metastasis. Possible predictors for lymphatic, vascular, and pleural invasion, and nodal metastasis and recurrence were investigated (Table 2). Revised maxSUV, GGO ratio, TDR, and BAC ratio were all significant determinants for predicting lymphatic permeation, vascular and pleural invasion, nodal metastasis, and recurrence. However, the odds ratios indicated that revised maxSUV and the BAC ratio revealed biological aggressive tumor grade more effectively than GGO ratio and TDR.

A significant difference in DFS was identified (Figure 3) between patients whose adenocarcinoma had revised maxSUV 2.5 or less (n = 343; 3-year DFS rate, 96%) and greater than 2.5 (n = 159; 3-year DFS rate, 77%; $P < .001$). We also found significant differences in DFS between patients whose adenocarcinoma had GGO ratios of

TABLE 1. Clinical characteristics of patients with cT1N0M0 adenocarcinoma (n = 502)

		Revised maxSUV		GGO ratio		TDR		BAC ratio	
	Patients (n = 502)	≤2.5/>2.5 (n = 343/159)	*P* value	≥20%/<20% (n = 304/198)	*P* value	≥30%/<30% (n = 346/156)	*P* value	≥30%/<30% (n = 304/198)	*P* value
Age (y) (means ±SD)	65.3 ± 9.6	65.3 ± 9.4/65.5 ±9.8	.8380	65.0 ± 9.3/65.9 ± 10.0	.2790	64.7 ± 9.4/66.7 ± 9.9	.0365	65.4 ± 9.5/65.3 ± 9.7	.9054
Gender									
Male	223	140/83	.0169	119/104	.0032	144/79	.0597	113/110	<.0001
Female	279	203/76		185/94		202/77		191/88	
CEA (ng/mL)									
≤5	449	321/128	<.0001	289/160	<.0001	324/125	<.0001	284/165	.0003
>5	53	22/31		15/38		22/31		20/33	
Tumor size (mm)									
T ≤20	290	218/72	.0001	183/107	.1723	213/77	.0104	180/110	.4178
<20 T ≤30	212	125/87		121/91		133/79		124/88	
Ly permeation									
positive	76	15/61	<.0001	13/63	<.0001	25/51	<.0001	12/64	<.0001
negative	426	328/98		291/135		321/105		292/134	
V invasion									
positive	92	16/76	<.0001	15/77	<.0001	23/69	<.0001	11/81	<.0001
negative	410	327/83		289/121		323/87		293/117	
P invasion									
positive	56	12/44	<.0001	10/46	<.0001	14/42	<.0001	6/50	<.0001
negative	446	331/115		294/152		332/114		298/148	
N metastasis									
positive	38	10/28	<.0001	8/30	<.0001	10/28	<.0001	5/33	<.0001
negative	464	333/131		296/168		336/128		299/165	

CEA, Carcinoembryonic antigen; *Ly,* lymphatic; *V,* blood vessel; *P,* pleural; *N,* lymph node; *maxSUV,* maximum standardized uptake value; *GGO,* ground-glass opacity; *TDR,* tumor disappearance rate; *BAC,* bronchioloalveolar carcinoma.

TABLE 2. Analysis of possible predictors for Ly factor, V factor, P factor, N factor, and recurrence status

Factors total (n = 502)	Favorable	Unfavorable	Odds ratio (95% CI)	*P* value
Positive Ly factor (n = 76)				
Revised maxSUV	≤2.5	>2.5	13.61 (7.41–25.01)	<.0001
GGO ratio	≥20%	<20%	10.45 (5.56–19.63)	<.0001
TDR	≥30%	<30%	6.24 (3.68–10.56)	<.0001
BAC ratio	≥30%	<30%	11.62 (6.07–22.25)	<.0001
Positive V factor (n = 92)				
Revised maxSUV	≤2.5	>2.5	18.71 (10.37–33.78)	<.0001
GGO ratio	≥20%	<20%	12.26 (6.78–22.17)	<.0001
TDR	≥30%	<30%	11.14 (6.57–18.88)	<.0001
BAC ratio	≥30%	<30%	18.44 (9.48–35.87)	<.0001
Positive P factor (n = 56)				
Revised maxSUV	≤2.5	>2.5	10.55 (5.39–20.68)	<.0001
GGO ratio	≥20%	<20%	8.90 (4.37–18.12)	<.0001
TDR	≥30%	<30%	8.74 (4.60–16.59)	<.0001
BAC ratio	≥30%	<30%	16.78 (7.03–40.03)	<.0001
Positive N factor (n = 38)				
Revised maxSUV	≤2.5	>2.5	7.12 (3.36–15.07)	<.0001
GGO ratio	≥20%	<20%	6.61 (2.96–14.74)	<.0001
TDR	≥30%	<30%	7.35 (3.47–15.56)	<.0001
BAC ratio	≥30%	<30%	11.96 (4.58–31.22)	<.0001
Positive recurrence (n = 29)				
Revised maxSUV	≤2.5	>2.5	7.71 (3.22–18.46)	<.0001
GGO ratio	≥20%	<20%	8.25 (3.09–22.01)	<.0001
TDR	≥30%	<30%	4.66 (2.11–10.28)	<.0001
BAC ratio	≥30%	<30%	10.84 (3.71–31.66)	<.0001

Ly, Lymphatic permeation; *V,* blood vessel invasion; *P,* pleural invasion; *N,* lymph node metastasis; *maxSUV,* maximum standardized uptake value; *GGO,* ground-glass opacity; *TDR,* tumor disappearance rate; *BAC,* bronchioloalveolar carcinoma.

GTS

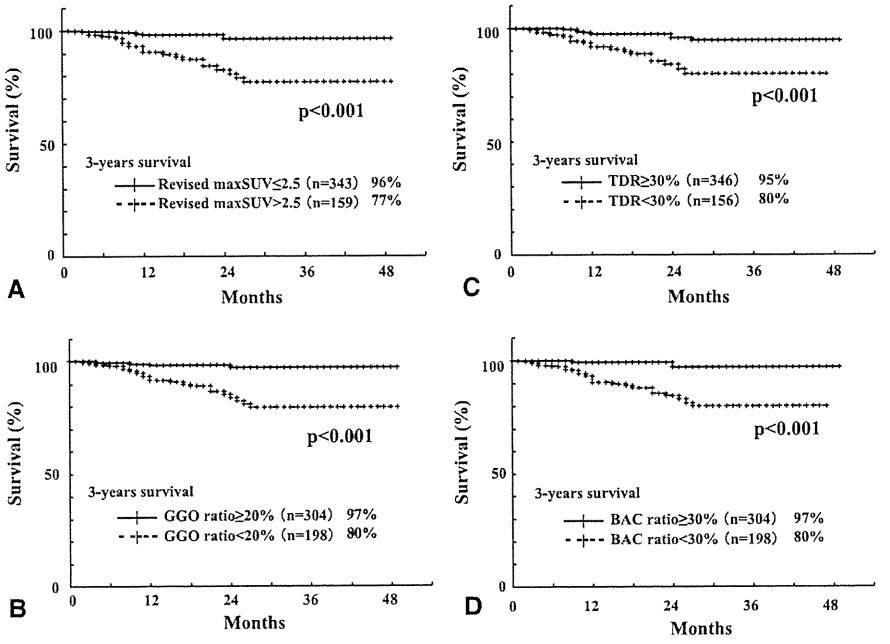

FIGURE 3. DFS curves according to grade of revised maxSUV (A), GGO ratio (B), TDR (C), and BAC ratio (D). *maxSUV,* Maximum standardized uptake value; *GGO,* ground-glass opacity; *TDR,* tumor disappearance rate; *BAC,* bronchioloalveolar carcinoma.

20% or more (n = 304; 3-year DFS rate, 97%) and less than 20% (n = 198; 3-year DFS rate, 80%; $P < .001$), between those whose adenocarcinoma had TDR 30% or more (n = 346; 3-year DFS rate, 95%) and less than 30% (n = 156; 3-year DFS rate, 80%; $P < .001$) and between those whose adenocarcinoma had BAC ratios of 30% or more (n = 304; 3-year DFS rate, 97%) and less than 30% (n = 198; 3-year DFS rate, 80%; $P < .001$). Revised maxSUV ($P = .016$) and GGO ($P = .024$) and pathologic BAC ($P = .005$) ratios were significant prognostic factors

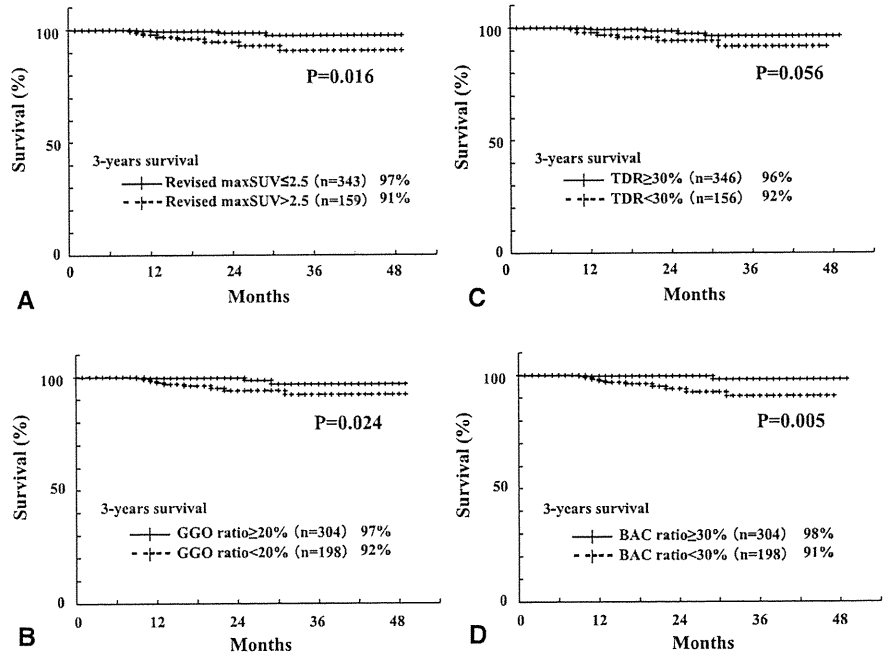

FIGURE 4. Overall survival curves according to grade of revised maxSUV (A), GGO ratio (B), TDR (C), and BAC ratio (D). *maxSUV,* Maximum standardized uptake value; *GGO,* ground-glass opacity; *TDR,* tumor disappearance rate; *BAC,* bronchioloalveolar carcinoma.

TABLE 3. Relationship between ground-glass opacity/tumor disappearance rate and revised maxSUV as predictors for Ly factor, V factor, P factor, N factor, and recurrence status

	Revised maxSUV	Ly permeation (+)/(-)	V invasion (+)/(-)	P invasion (+)/(-)	N metastasis (+)/(-)	Recurrence (+)/(-)
GGO ≤50% and TDR ≤50%	≤1.5	2/46	1/47	3/45	0/48	0/48
(n = 259)	(n = 48)	(4%)	(2%)	(6%)	(0)	(0)
	<1.5 ≤2.5	10/58	14/54	8/60	8/60	3/65
	(n = 68)	(15%)	(21%)	(12%)	(12%)	(4%)
	2.5<	59/84	73/70	43/100	27/116	22/121
	(n = 143)	(41%)	(51%)	(30%)	(19%)	(15%)
>50% GGO or >50% TDR	≤1.5	2/178	1/179	0/180	1/179	2/178
(n = 243)	(n = 180)	(1%)	(1%)	(0)	(1%)	(1%)
	<1.5 ≤2.5	1/46	0/47	1/46	1/46	2/45
	(n = 47)	(2%)	(0)	(2%)	(2%)	(4%)
	2.5<	2/14	3/13	1/15	1/15	0/16
	(n = 16)	(13%)	(19%)	(6%)	(6%)	(0)

maxSUV, Maximum standardized uptake value; *Ly,* lymphatic; *V,* blood vessel; *P,* pleural; *N,* lymph node; *GGO,* ground-glass opacity; *TDR,* tumor disappearance rate.

for overall survival, whereas TDR ($P = .056$) was marginally significant (Figure 4).

We examined the relationships between HRCT findings and maxSUV for predicting tumor invasiveness, nodal metastasis, and recurrence (Table 3). Generally, solid tumors on HRCT with GGO 50% or less and TDR 50% or less had high maxSUV and were more frequently associated with high malignant grade, nodal metastasis, and recurrence. However, solid tumors with lower maxSUV were associated with low malignant grade and far less nodal metastasis and recurrence. Among patients with tumors showing GGO 50% or less and TDR 50% or less, 19% and 15% of those with a revised maxSUV greater than 2.5 had nodal metastasis and recurrence, respectively,

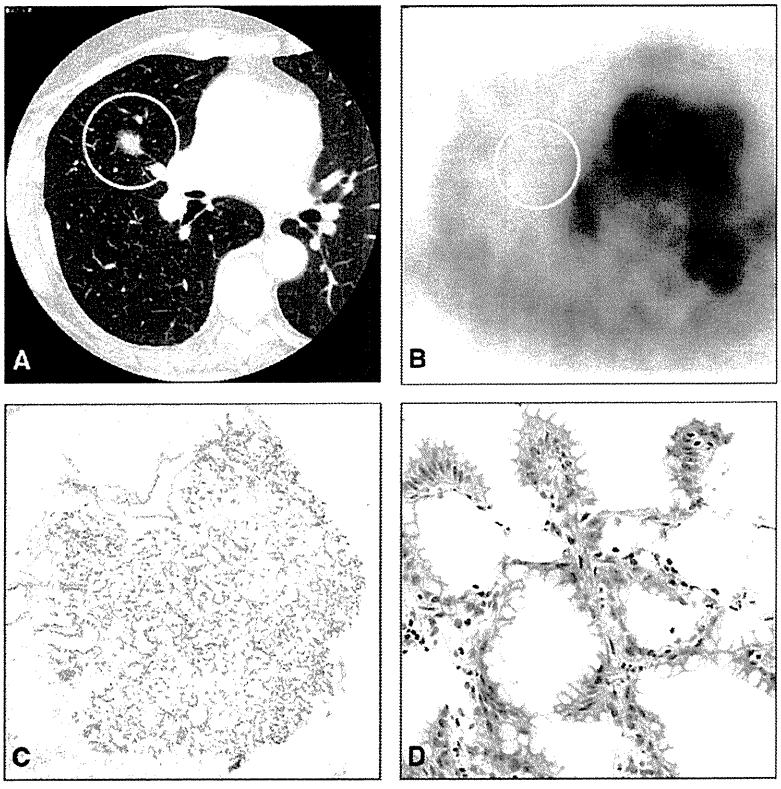

FIGURE 5. Tumor (1.5 cm in diameter) located at right middle lobe. A, HRCT findings show GGO ratio of 5%. B, PET/CT findings show no accumulation. Microscope findings show BAC with mucin formation (C and D, staining with hematoxylin–eosin at ×25 and ×200 magnification, respectively).

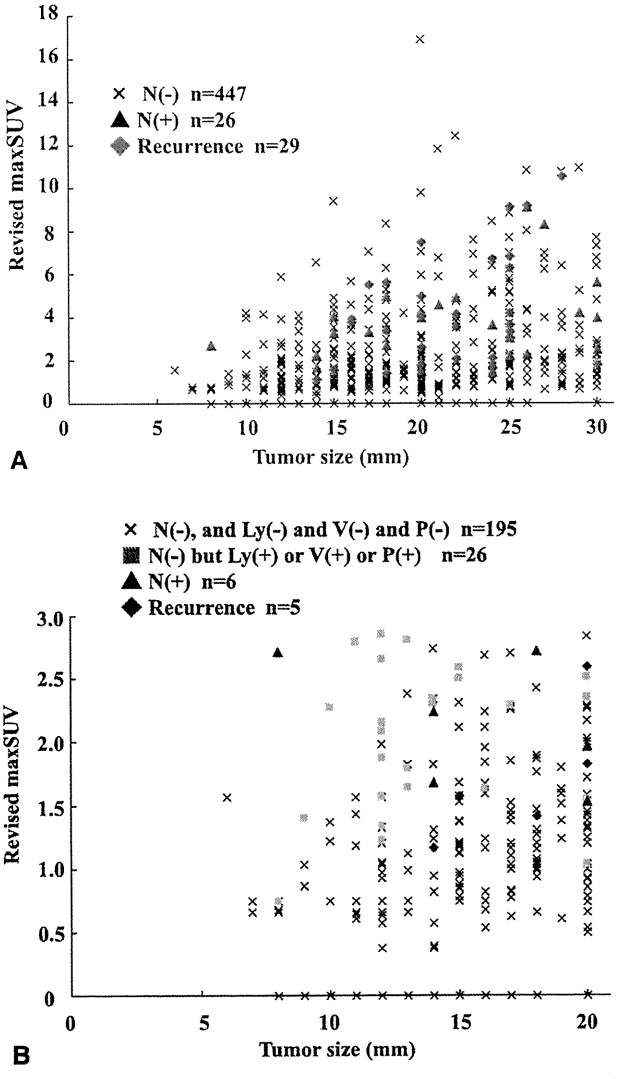

FIGURE 6. Relationship between tumor size and revised maxSUV level in cT1N0M0 adenocarcinomas. A, All patients. B, Tumor size ≤ 20 mm and revised maxSUV ≤ 3.0. Nodal metastasis (*triangles*); recurrence (*rhombi*); lymphatic, vascular, or pleural invasion without nodal metastasis (*squares*). *maxSUV,* Maximum standardized uptake value; *N,* lymph node; *Ly,* lymphatic; *V,* blood vessel; *P,* pleural.

whereas those with tumors showing revised maxSUV 1.5 or less had neither nodal metastasis nor recurrence.

DISCUSSION

The frequency of identifying small lung cancers has recently increased since CT and enhanced scanning have become routine procedures and surgeons have thus been able to assess the advantages of sublobar resection, such as radical segmentectomy instead of lobectomy.[2,3] The biological malignancy of small adenocarcinoma has generally been evaluated on the basis of HRCT findings. The specificity, sensitivity, and accuracy of radiologic diagnoses with HRCT on lymphatic/vessel invasion and nodal involvement of clinical T1N0M0 adenocarcinoma have been examined in a large prospective study (JCOG0201).[12] The conclusions failed to corroborate predetermined criteria using GGO ratio and TDR for specificity, and thus applicants for radical sublobar resection could not be suitably confirmed on the basis of criteria generated from HRCT findings. Therefore, the development of a novel tool that surpasses the diagnostic ability of HRCT is a current challenge.

Phase III randomized trials of standard lobectomy versus experimental limited resection for small (≤2 cm in diameter) peripheral non–small cell lung cancers are ongoing in the United States (CALGB-140503) and in Japan (JCOG0802/WJOG4607L). Because the biological behavior of several types of small lung cancers is aggressive, to detect indolent lung cancers preoperatively with radiographic imaging is important for the standardization of sublobar resection, although accurate radiographic definition of tumor extension and metastasis is challenging. We previously demonstrated that maxSUV on FDG-PET/CT is a potentially promising parameter of the degree of malignancy among cT1N0M0 lung adenocarcinoma.[7,8] However, relatively few patients were analyzed and postoperative survival data were obtained during a short period. We therefore performed an extended, larger multicenter study. To our knowledge, a large scale multi-institutional study of malignant tumor grade analyzed using PET/CT has not been reported.

The present analyses revealed that adenocarcinoma with high maxSUV and low GGO ratio, TDR, or BAC ratio is more closely associated with lymphatic, vessel, pleural invasion, lymph node metastasis, and recurrence. We also found a closer association between serum CEA levels and maxSUV, GGO ratio, TDR, and BAC ratio, which is preoperatively vital in uncovering patients at high risk of potential advanced disease.[13,14] High maxSUV was also a poor prognostic determinant for DFS and overall survival. These outcomes suggested that maxSUV can be a realistic surrogate marker of tumor malignancy grade and that FDG-PET/CT in addition to HRCT is a potent prognostic modality with which to detect patients at high risk of recurrence after curative resection of small adenocarcinoma.

Because PET/CT imaging reflects metabolic activity as glucose metabolism whereas HRCT generates only anatomic images, findings of PET/CT could be more powerful clinical predictors of biological tumor performance than those of HRCT. Most solid tumors on HRCT have high maxSUV and aggressive malignant behavior, whereas solid tumors with lower maxSUV were less aggressive. Figure 5 shows a mucinous BAC with indolent behavior that appeared as a solid tumor on HRCT with no accumulation on PET/CT.

We analyzed the association between tumor size and maxSUV in cT1N0M0 adenocarcinoma (Figure 6). A larger

tumor was associated with a higher maximum SUV, and both size and maxSUV can predict tumor invasiveness, nodal metastasis, and recurrence. The figures show a notable tendency of small adenocarcinoma with high maxSUV to have more malignant features than larger adenocarcinoma with low maxSUV.

One of the major limitations of multicenter trials using PET is the wide variation in SUV among institutions. Many factors, such as preparation procedures, scan acquisition, image reconstruction, and data analysis affect SUV,[15,16] although semiquantitative SUV in patients with cancer is extensively applied to diagnose, stage, and evaluate therapeutic effectiveness.[4-6] Westerterp and colleagues[17] reported that a discrepancy in SUV of up to 30% among institutions could create a significant problem for multicenter studies. Inter-institutional variability in SUV obtained in the present study was minimized using an anthropomorphic body phantom. Therefore, quantitative SUVs adjusted by phantom studies can be dependable, and such correction will help to overcome one major limitation of multicenter of PET studies.

CONCLUSIONS

The findings of HRCT and FDG-PET/CT are important to select therapeutic strategies for treating c-stage IA adenocarcinoma of the lung, and maxSUV on FDG-PET/CT is an especially significant preoperative predictor for surgical outcomes. Sublobar resection might be performed in patients with adenocarcinoma with maxSUV 1.5 or less, and lymphadenectomy is required for tumors with maxSUV greater than 1.5.

References

1. Ginsberg RJ, Rubinstein LV. Randomized trial of lobectomy versus limited resection for T1N0 non-small cell lung cancer. Lung Cancer Study Group. *Ann Thorac Surg*. 1995;60:615-22.
2. Okada M, Koike T, Higashiyama M, Yamato Y, Kodama K, Tsubota N. Radical sublobar resection for small-sized non-small cell lung cancer: a multicenter study. *J Thorac Cardiovasc Surg*. 2006;132:769-75.
3. Nakayama H, Yamada K, Saito H, Oshita F, Ito H, Kameda Y, et al. Sublobar resection for patients with peripheral small adenocarcinomas of the lung: surgical outcome is associated with features on computed tomographic imaging. *Ann Thorac Surg*. 2007;84:1675-9.
4. Pieterman RM, van Putten JW, Meuzelaar JJ, Mooyaart EL, Vaalburg W, Koëter GH, et al. Preoperative staging of non-small-cell lung cancer with positron-emission tomography. *N Engl J Med*. 2000;343:254-61.
5. Vansteenkiste J, Fischer BM, Dooms C, Mortensen J. Positron-emission tomography in prognostic and therapeutic assessment of lung cancer: systematic review. *Lancet Oncol*. 2004;5:531-40.
6. Juweid ME, Cheson BD. Positron-emission tomography and assessment of cancer therapy. *N Engl J Med*. 2006;354:496-507.
7. Okada M, Tauchi S, Iwanaga K, Mimura T, Kitamura Y, Watanabe H, et al. Associations among bronchioloalveolar carcinoma components, positron emission tomographic and computed tomographic findings, and malignant behavior in small lung adenocarcinomas. *J Thorac Cardiovasc Surg*. 2007;133:1448-54.
8. Nakayama H, Okumura S, Daisaki H, Kato Y, Uehara H, Adachi S, et al. Value of integrated positron emission tomography revised using a phantom study to evaluate malignancy grade of lung adenocarcinoma: a multicenter study. *Cancer*. 2010;116:3170-7.
9. Mawlawi O, Podoloff DA, Kohlmyer S, Williams JJ, Stearns CW, Culp RF, et al. Performance characteristics of a newly developed PET/CT scanner using NEMA standards in 2D and 3D modes. *J Nucl Med*. 2004;45:1734-42.
10. Shimizu K, Yamada K, Saito H, Noda K, Nakayama H, Kameda Y, et al. Surgically curable peripheral lung carcinoma. Correlation of thin-section CT findings with histologic prognostic factors and survival. *Chest*. 2005;127:871-8.
11. Delbeke D, Coleman RE, Guiberteau MJ, Brown ML, Royal HD, Siegel BA, et al. Procedure guideline for tumor imaging with 18F-FDG PET/CT 1.0. *J Nucl Med*. 2006;47:885-95.
12. Suzuki K, Koike T, Shibata T, Kusumoto M, Asamura H, Nagai K, et al. Evaluation of radiologic diagnosis in peripheral clinical IA lung cancers. A prospective study for radiological diagnosis of peripheral early lung cancer (JCOG0201). *J Clin Oncol*. 2006;24:7220.
13. Okada M, Nishio W, Sakamoto T, Uchino K, Yuki T, Nakagawa A, et al. Prognostic significance of perioperative serum carcinoembryonic antigen in non-small cell lung cancer: analysis of 1,000 consecutive resections for clinical stage I disease. *Ann Thorac Surg*. 2004;78:216-21.
14. Okada M, Nishio W, Sakamoto T, Uchino K, Yuki T, Nakagawa A, et al. Effect of histologic type and smoking status on interpretation of serum carcinoembryonic antigen value in non-small cell lung carcinoma. *Ann Thorac Surg*. 2004;78:1004-9.
15. Boellaard R, Oyen WJG, Hoekstra CJ, Hoekstra OS, Visser EP, Willemsen AT, et al. The Netherlands protocol for standardisation and quantification of FDG whole body PET studies in multi-centre trials. *Eur J Nucl Med Mol Imaging*. 2008;35:2320-33.
16. Boellaard R, Krak NC, Hoekstra OS, Lammertsma AA. Effects of noise, image resolution, and ROI definition on the accuracy of standard uptake values: a simulation study. *J Nucl Med*. 2004;45:1519-27.
17. Westerterp M, Pruim J, Oyen W, Hoekstra O, Paans A, Visser E, et al. Quantification of FDG PET studies using standardized uptake values in multicenter trials: effects of image reconstruction, resolution and ROI definition parameters. *Eur J Nucl Med Mol Imaging*. 2007;34:392-404.

GTS